Available online at www.sciencedirect.com
ScienceDirect
Trans. Nonferrous Met. Soc. China 25(2015) 112−121
Transactions of Nonferrous Metals Society of China
www.tnmsc.cn

Research progress of Ag_3PO_4-based photocatalyst: Fundamentals and performance enhancement

Yun-zhu MA, Fan CHENG, Wen-sheng LIU, Juan WANG, Yi-kai WANG

State Key Laboratory of Powder Metallurgy, Central South University, Changsha 410083, China

Received 10 February 2014; accepted 12 May 2014

Abstract: Ag_3PO_4 is found to be a highly efficient photocatalyst and receives great attention. The high activity of the photocatalyst is credited to the intrinsic electronic structure. The morphology control and nano-composite fabrication are used to improve the performance and practicability. This paper reviews the structure, properties and some theoretical aspects of Ag_3PO_4 single crystal. Also, the major strategies, namely the morphology control and hetero-nanostructure construction, as ways to improve the performance of Ag_3PO_4-based photocatalysts, are summarized with the aid of some typical instances.

Key words: Ag_3PO_4-based photocatalyst; electronic structure; morphology control; hetero-structure construction; preparation; photocatalytic activity

1 Introduction

Pollutants released by both civilian and military sectors have been imposing great threats on the water quality worldwide [1−3]. Thus, on behalf of the sustainable development of human society, large amount of scientific and technological efforts are paid toward water purification. Among those strategies, heterogeneous semiconductor photocatalysis has been recognized generally as a promising green route because it paves a possible way of utilizing the solar irradiation or artificial indoor illumination to decompose contaminants [4].

Since FUJISHIMA [5] discovered the photocatalytic phenomenon of TiO_2 electrode in 1972, TiO_2-based photocatalysts have been most comprehensively studied. TiO_2 has the merits of low cost, strong redox capacity, relatively high activity and stability, etc [5−8]. However, due to such intrinsic limitations as wide band gap (3−3.2 eV), it is not adequate for all conditions especially under visible light irradiation [9−11]. Though doping can decrease the band gap, it will simultaneously introduce states that act as combining centers [12−16], which lowers the quantum efficiency. Thus, the development of novel visible light responsive photocatalysts has become an urgent issue.

Simple metal oxides (Fe_2O_3, WO_3, SnO_2, Bi_2O_3, etc) [17−20], multi-metal oxides (Bi_2WO_6, $BiVO_4$, $CaBi_2O_4$, $InVO_4$, etc) [21−24], solid solutions (ZnO_x−GaN_{1-x}, $NaNbO_3$−$AgNbO_3$, $BiTa_{1-x}Nb_xO_4$, etc) [25−27] have been tried in terms of obtaining the desired band gap to achieve visible absorption. Among these, Ag^+-based multi-metal oxides, especially those derived by combining Ag_2O and oxides of p-block elements (Ag_3PO_4, $AgAlO_2$, $AgGaO_2$, etc), were found to be promising. The improved photocatalytic performance can be credited to their similar electronic structures [28−30].

As a unique one, Ag_3PO_4 is so far the only compound that incorporates nonmetallic p-block specie into Ag_2O. More importantly, it possesses ultra-high photocatalytic activity in O_2 evolution and organic contaminant degradation [31]. Since YI et al [31] first used Ag_3PO_4 for photocatalysis and demonstrated the high activity, lots of researches have been devoted to Ag_3PO_4-based photocatalysts. Thus, a clear and complete summery of the present progress is essential. In this review, the structure, properties and some theoretical aspects of Ag_3PO_4 single crystal are introduced, while the major strategies, namely the morphology control and hetero-nanostructure construction, are concluded with the aid of some reliable examples.

2 Structure and properties of Ag_3PO_4

Ag_3PO_4 possesses a cubic crystal structure. The

Corresponding author: Yun-zhu MA; Tel: +86-731-88877285; E-mail: zhuzipm@mail.csu.edu.cn
DOI: 10.1016/S1003-6326(15)63585-3

space group is $P\bar{4}3n$. As Fig. 1 [32] illustrated, the PO_4 tetrahedron and AgO_4 tetrahedron constitute the lattice [33,34]. By theoretical optimization, the cell parameters obtained are $a=b=c=6.010$ Å and $\alpha=\beta=\gamma=90°$ [35]. This nearly fits with the experimental data of $a=b=c=6.026$ Å and $\alpha=\beta=\gamma=90°$.

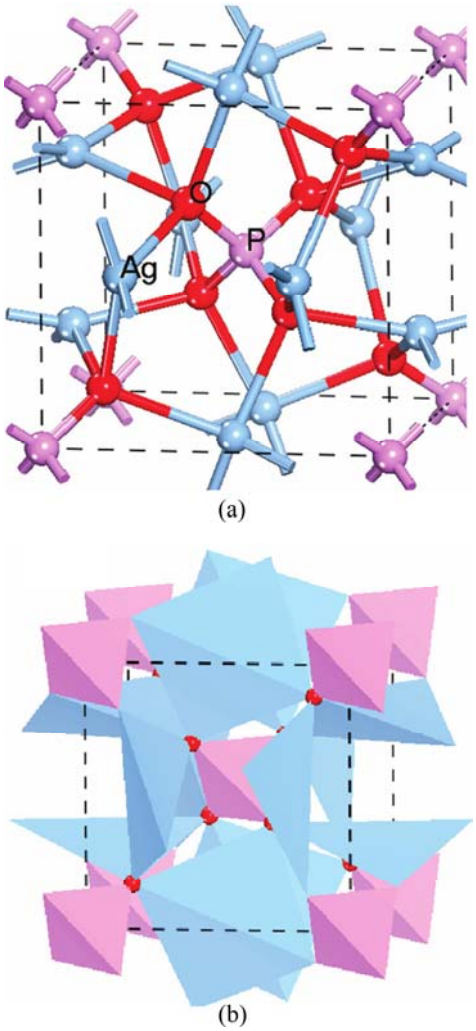

Fig. 1 Illustration of crystal structure of Ag_3PO_4 with ball-stick(a) and polyhedron(b) (Red, purple, and blue spheres represent O, P, and Ag atoms, respectively [32])

To understand the origin of the high photocatalytic property of Ag_3PO_4, a comprehension of the electronic structure of the compound is needed. Experimentally, Ag_3PO_4 possesses an indirect band-gap of 2.36 eV as well as a direct transition of 2.43 eV, which was deduced from the ultraviolet-visible diffuse reflectance spectrum (Fig. 2) [31]. Thus, Ag_3PO_4 is able to absorb irradiation with a wavelength shorter than 530 nm, well extending into the visible region.

Also, theoretical studies were carried out. UMEZAWA et al [28] employed the DFT-based methods to reveal that due to the strong P—O bonds of PO_4 tetrahedral units, the covalent nature of Ag—O bonds is

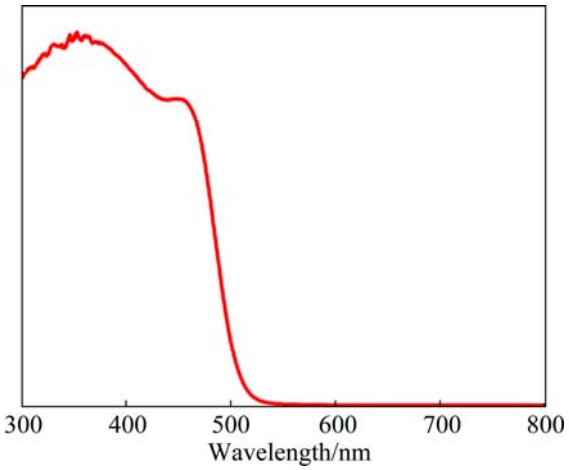

Fig. 2 Ultraviolet-visible diffusive reflectance spectrum of Ag_3PO_4 samples [31]

weakened. This impairs the Ag d and O p states to blend. Thus, the d character is excluded from the conduction-band minimum (CBM), remaining highly dispersive Ag s—Ag s hybrid bands. This leads to a small effective mass of the electron, which is advantageous for the carrier transfer to surface. MA et al [33] used first-principle DFT combined with the LDA+U formalism to show that Ag_3PO_4 has a large dispersion of conduction band, which facilitates the separation of charge carriers. Moreover, high concentration of Ag vacancies in Ag_3PO_4 lattice has a significant effect on the separation of electron−hole pairs and optical absorbance in the visible-light region. In addition to the calculations performed by the above two studies, LIU et al [35] used hybrid density functional method to more precisely get the electronic structure of Ag_3PO_4 photocatalyst (Figs. 3 and 4). The results reveal a band gap of 2.43 eV, which agrees well with the experimental result. The conduction bands are credited to Ag 5s and 5p states, while the valence bands mainly consist of O 2p and Ag 4d states. The VBM potential was 2.67 eV (vs normal hydrogen electrode), which indicates an adequate driving force for water oxidation or pollutants degradation.

On the other hand, the photocatalytic redox mechanism is illustrated with reference to CBM, VBM and the potentials of the relevant redox pairs (Fig. 5) [31]. It is evident that Ag_3PO_4 is able to decompose organic pollutants or split water to produce O_2 when $AgNO_3$ is present as the sacrificial agent. Moreover, Ag_3PO_4 shows a much higher photocatalytic activity in comparison with WO_3, $BiVO_4$, etc [28,31,32], which implies that Ag_3PO_4 is potentially a highly efficient photocatalyst. Consequently, much attention has been paid to the improvement of the property of Ag_3PO_4 (morphology control and hetero-structure fabrication).

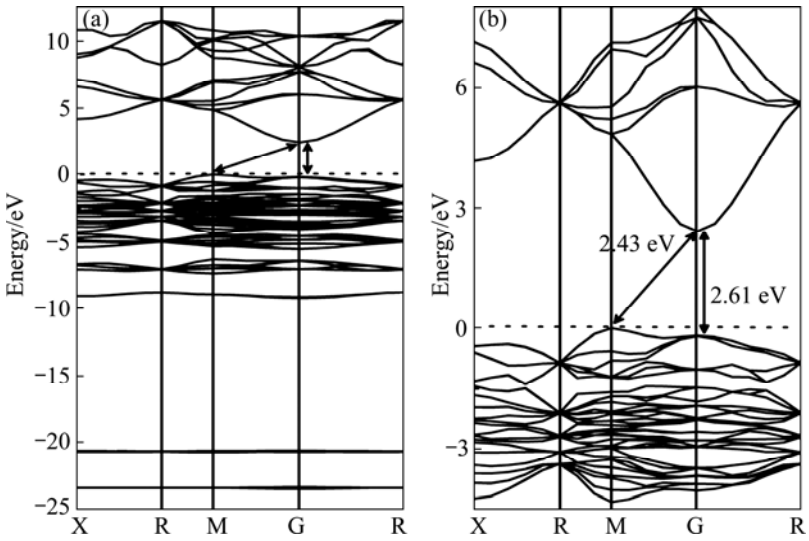

Fig. 3 Band structure of Ag_3PO_4 calculated using PBE0 approach (a) and magnified view of band structure near Fermi level (b) [35]

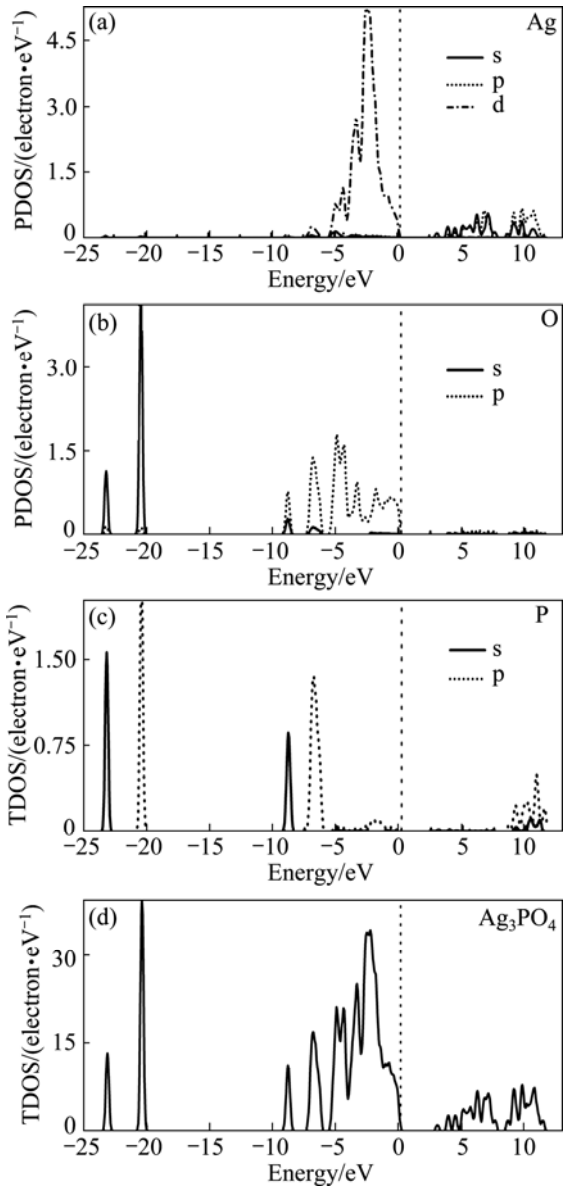

Fig. 4 TDOS and PDOS of Ag_3PO_4 using PBE0 approach [35]

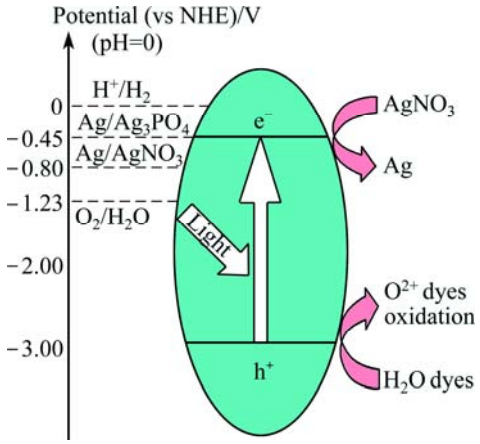

Fig. 5 Photon induced oxidation over Ag_3PO_4 under visible light as well as illustration of redox potentials of Ag_3PO_4 [31]

3 Morphology control strategy

As a common sense in the field of photocatalysis, the morphology (size, shape and kind of exposed facets, etc) of the photocatalysts has an influence on the efficiency and activity [4]. This also applies, within expectation, to the Ag_3PO_4-based materials. Since Ag_3PO_4 is a promising photocatalyst, lots of researches have been conducted to the morphology tuning. Such novel shapes as branch, tetrapod, nanorod, triangular prism [36], pine tree [37] and porous microcubes [38] are successfully obtained. Generally, those preparation methods involve precipitation (with the aid of Ag^+−ligant complex, organic additives or templates) [37,39], chemical or electrochemical oxidation of metallic Ag into Ag^+ (subsequently captured by PO^{4-}) [40], ligant-assisted anion exchange process [41] and hydrothermal synthesis [42] etc. Except for modulating the inner conditions of the reactions, those outside factors like

ultrasound were also demonstrated to be influential to the morphology [36].

WANG et al [43] first managed to synthesize uniform tetrapod-like Ag_3PO_4 microcrystals (T-Ag_3PO_4) with a simple hydrothermal method without adding any template or surfactant. The precursor was phosphoric acid while the pH value of the reaction system was tuned by urea. By varying the amount of the urea, reaction time and temperature, the morphology of the product was successfully tuned. As the SEM images (Figs. 6(a) and (b)) shown, four arms of the tetrapod are cylindrical microrods with an average diameter of 5 μm and a length of 15−30 μm. As the XRD patterns shown (Fig. 6(c)), the intensity ratios of (110)/(200) and (222)/(321) for T-Ag_3PO_4 are 2.9 and 1.6, which are remarkably higher than those (0.56 and 0.9) of the irregular counterpart, respectively. From the XRD pattern, the high exposing rate of the (110) facet is demonstrated. The origin for higher intensity ratio of (110)/(200) is credited to the high surface energy of (110). The activity of the product was demonstrated in RhB degradation (Fig. 6(d)). In comparison with N-doped TiO_2, the Ag_3PO_4 samples exhibited higher catalytic activities, while the T-Ag_3PO_4 possessed the highest activity. The highest activity of T-Ag_3PO_4 was resulted from the higher surface energy of (110) facets than those of (200) facets.

A special example, with regard to the preparation method, is worth mentioning. JIAO et al [44] fabricated various shaped Ag_3PO_4 microcrystals based on the heteroepitaxial growth procedure, in which different seeds were added into the reaction system before precipitation happened. This is a procedure well recognized in the field of nano fabrication, in which the nucleation and crystal growth are separated in terms of space and time [45]. Figure 7 [44] illustrates the preparation procedure as well as the SEM images of the products. Actually, considering the fact that the structure diversity of the crystal nucleus will lead to drastically different shaped products, the usage of pure single sorts of seeds are beneficial to forming pure, uniform shaped crystals as well as to obtaining the desired morphology.

Though an absence of comparison in terms of activity between individual literatures, nearly all of them showed an enhanced reaction rate with regard to the spherical counterpart and N-doped TiO_2. Considering the large amount of the researches, some of the reliable and representative instances are listed in Table 1 with regard to the morphology, preparation method and photocatalytic activity.

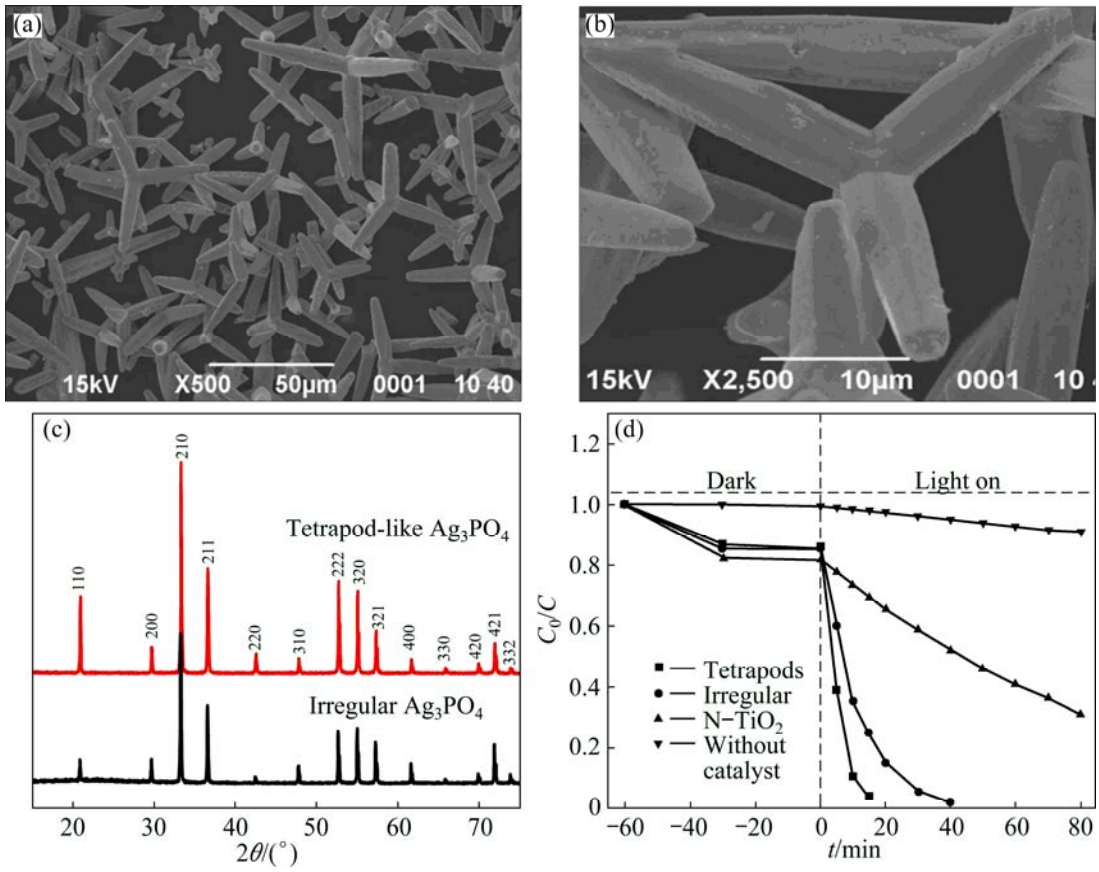

Fig. 6 SEM images of T-Ag_3PO_4 at different magnifications (a, b), XRD patterns of tetrapod-like and irregular Ag_3PO_4 (c) and degradation of RhB with tetrapod-like Ag_3PO_4, irregular Ag_3PO_4 and N-doped TiO_2 under visible-light (λ>420 nm) (d) [43]

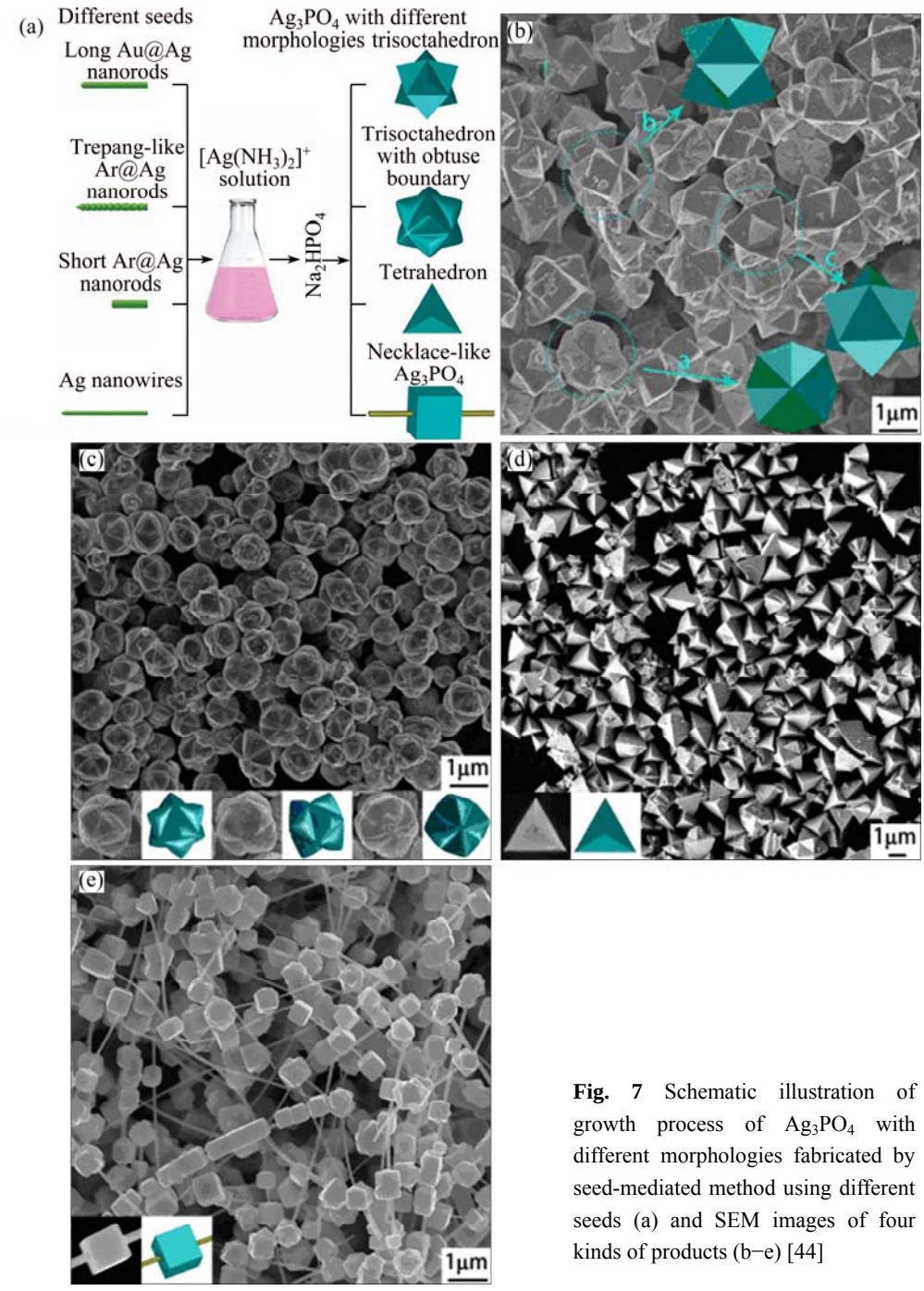

Fig. 7 Schematic illustration of growth process of Ag_3PO_4 with different morphologies fabricated by seed-mediated method using different seeds (a) and SEM images of four kinds of products (b−e) [44]

4 Hetero-nanostructure construction

Fabricating hetero-structure is a common strategy to enhance the activity of photocatalysts as well as to overcome some application barriers [4]. Such attempts were also made in the case of Ag_3PO_4. Ag_3PO_4-based composite photocatalysts including TiO_2/Ag_3PO_4 (decreasing Ag content to reduce cost) [48], Fe_3O_4/Ag_3PO_4 (magnetic separable) [49], $In(OH)_3/Ag_3PO_4$ (enhancing absorption by tuning surface electric property) [50], Ag_3PO_4/carbon nanotube-stabilized pickering emulsion (enhancing activity by surface-chemical design of novel micro-reaction system) [51], Ag_3PO_4-graphene [52], $Ag@(Ag_2S/Ag_3PO_4)$ (facilitating migration of charge carriers) (enhancing activity via synergistic effect of Ag and Ag_2S) [53], AgX/Ag_3PO_4 (improving stability via core-shell structure) [54] and so forth have been successfully synthesized and studied. Each of the synthesized photocatalysts shows exclusive characters (described in the brackets behind) as well as common features shared with others like the promotion of charge carrier separation, increase of surface area and so forth. To see the literatures as a

Table 1 Preparation and photocatalytic properties of Ag_3PO_4 with different morphologies

Morphology	Preparation method	Condition for Photocatalytic activity test	Activity	Reference photocatalyst and activity	Enhancement factor	Ref.
A: Rhombic dodecahedron	Precipitation reaction between CH_3COOAg and Na_2HPO_4	Degradation of MO under visible light (λ>420 nm)	Complete degradation (CD): ~ 4 min	Spherical Ag_3PO_4; CD: ~ 28 min	7	[39]
B: Cube	Precipitation: reaction between $[Ag(NH3)_2]^+$ and Na_2HPO_4	Degradation of MO under visible light (λ>420 nm)	CD: ~ 14 min	Spherical Ag_3PO_4; CD: ~ 28 min	2	[39]
Porous microcubes	Na_3Cit assisted synthesis: Formation and transformation of Ag_3Cit	Degradation of RhB under visible light (λ> 420 nm)	CD: ~ 25 min (sample obtained with reaction time of 5 h)	solid Ag_3PO_4 powders; CD: ~ 50 min	2	[38]
Tetrahedral submicro-crystals	Reaction of Ag foils with H_2O_2 and NaH_2PO_4	Degradation of MO under visible light	CD: 6 min	Ag_3PO_4 cubes; CD: 14 min	2.33	[40]
Concave microcrystals	electrochemical oxidation of bulk silver sheet	Degradation of MB under visible light (λ>400 nm)	CD: 30 min	A: N-doped 20% TiO_2 in 30 min); B: Irregularly-shaped particles, 42% in 30 min	A: 5 B: 2.38	[46]
A: Branched B: Tetrapod C: Nanorod D: Triangular-prism	Precipitation: reaction between DMF−Ag^+−H_2O complex and PO_4^{3-} (A: static, B: static, followed by Ostwald ripening; C: ultrasonic, D: ultrasonic, followed by Ostwald ripening)	Degradation of MB under visible light	Branched (100 % in 30 min) >nanorod-shaped (90% in 30 min) > irregular spherical (80 % in 30 min) > tetrapod > triangular-prism (62 % in 30 min)	Irregular spherical, 80 % in 30 min	A: 1.25 B: 1.125 C: − D: −	[36]
Two-dimensional dendritic	Reacting Ag nanowires with H_2O_2 and NaH_2PO_4 (adding 0.3 mol/L PVP)	Degradation of RhB under visible light (λ > 420 nm)	CD: 3 min	Ag_3PO_4 obtained without adding PVP; CD: 9 min	3	[47]

whole, one would be puzzled by the amount as well as the void of a complete comparison between the activities of the photocatalysts (variation of testing condition). To simplify, only selective instances are briefly introduced, while others are listed in Table 2.

HOU et al [58] prepared graphene-supported Ag_3PO_4/Ag/AgBr via photoassisted deposition−precipitation method. This was followed by subsequent hydrothermal treatment. Under the irradiation of visible light, the O_2-evolution rate of the nano-composite was two times of that of the bare Ag_3PO_4 powder. Compared with unsupported Ag_3PO_4/Ag/AgBr, graphene supported bare Ag_3PO_4 and Ag/AgBr, it also performed improved activity (Fig. 8). The depletion of the conduction band electrons of Ag_3PO_4, downshift of the Ag_3PO_4 valence band influenced by silver and charge transferring onto the graphene support were responsible for the enhanced activity (Fig. 9).

Another special case, in terms of the preparation method, is the work of YU et al [59]. Necklace-like Ag_3PO_4– polyacrylonitrile (PAN) hetero-nanofibers were successfully fabricated through electrospinning technique (Fig. 10). The product exhibited excellent photocatalytic activities for the degradation of organic contaminants under visible light irradiation. By tuning the mass ratio (between Ag_3PO_4 and PAN) and applied voltage, the morphology of the product can be changed correspondently. Since electrospun polyacrylonitrile is used in clothing production, this research implies a possibility to make the clothing material photocatalytic self-cleanable.

5 Conclusion and perspective

In summery, Ag_3PO_4, with characteristic electronic structure, is an efficient photocatalyst, which can harness the visible light to oxidize water as well as decompose organic pollutants in aqueous solution. From the point view of quantum chemistry, Ag_3PO_4 is the result of inserting a nonmetallic p block element-phosphorus-into the simple narrow band gap Ag_2O semiconductor. The introduction of p block elements (Al, Ga, Ge, As, and Sb, etc) into Ag_2O implicates a new strategy of designing high efficiency photocatalyst. The two typical strategies,

Table 2 Preparation and photocatalytic properties of Ag_3PO_4-based hetero-structures

Hetero-structure	Preparation method	Condition for photocatalytic test	Activity	Reference photocatalyst and activity	Enhancement factor	Ref.
$Ag_3PO_4/In(OH)_3$	In-situ deposition-precipitation	Degradation of RhB under simulation solar irradiation	CD: 2 min	Bare Ag_3PO_4; CD: 9 min	4.5	[51]
Ag_3PO_4−graphene	Hydrothermal method	Degradation of RhB under visible light (λ > 420 nm)	100 % in 2 min	Ag_3PO_4 polyhedra; 100 % in 4 min	2	[53]
Ag_3PO_4-MWNTs stabilized pickering emulsion	Precipitation and simple mixture under sonication	Degradation of MB under visible light	k: 0.48 min^{-1}	Raw Ag_3PO_4 nanoparticles in the solution-dispersed system; k: 0.24 min^{-1}	2	[52]
AgX/Ag_3PO_4 (X=Cl, Br, I)	Precipitation followed by ion-exchange method	Degradation of MO under visible light	CD: $AgCl/Ag_3PO_4$, 30 min; $AgBr/Ag_3PO_4$, 5 min; AgI/Ag_3PO_4, 10 min	Bare Ag_3PO_4; CD: 55 min	Cl: 1.83; Br: 11; I: 5.5	[59]
Ag_3PO_4/TiO_2	In-situ precipitation method	Degradation of MB under visible light	CD: 9 min	Bare Ag_3PO_4; CD: 15 min	1.67	[49]
Ag_3PO_4/CQDs CQDs/Ag/Ag_3PO_4	In-situ precipitation(dark) In-situ precipitation (irradiated with light)	A: Degradation of MO under visible light B: Degradation of MO under visible light	A, CD: 30 min B, CD: 10 min	Bare Ag_3PO_4; CD: 58 min	A: 1.93 B: 5.8	[56]
g-C_3N_4–Ag_3PO_4	In-situ precipitation	Degradation of MO under visible light	100 % in 20 min	60 % in 20 min	3.5	[57]
Ag@(Ag_2S/Ag_3PO_4)	Anion-exchange method and subsequent calcination treatment	Degradation of Rh B under visible light	CD: 17 min	CD: 150 min	8.82	[54]

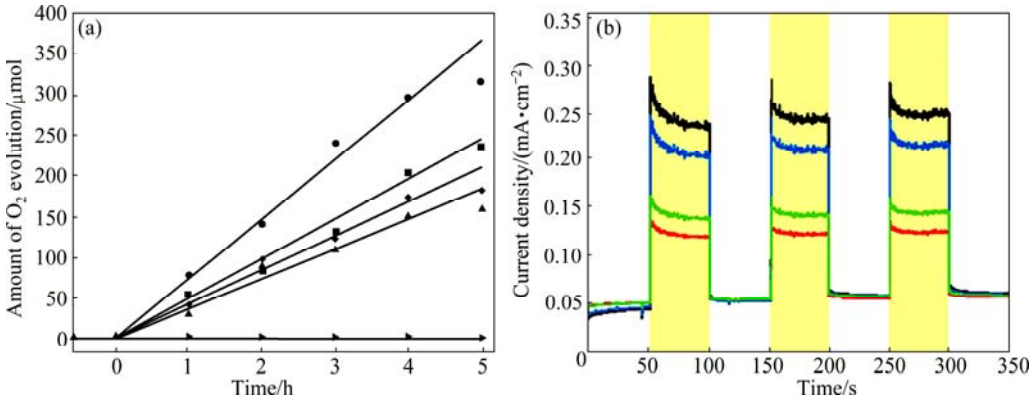

Fig. 8 Photocatalytic O_2 evolution under visible light irradiation (wavelength > 420 nm) over bare Ag/AgBr, Ag_3PO_4, Ag_3PO_4/RGO, Ag_3PO_4/Ag/AgBr, and Ag_3PO_4/Ag/AgBr/RGO (from bottom to top) (a) and transient photocurrent responses of electrodes functionalized with Ag_3PO_4-based materials in the same order (bottom to top) as in panel (b) (Measurements proceeded in a 0.01 mol/L Na_2SO_4 aqueous solution under visible light irradiation (wavelength > 420 nm, I_0=64 mW/cm^2) at 0.5 V (vs SCE) bias [58]

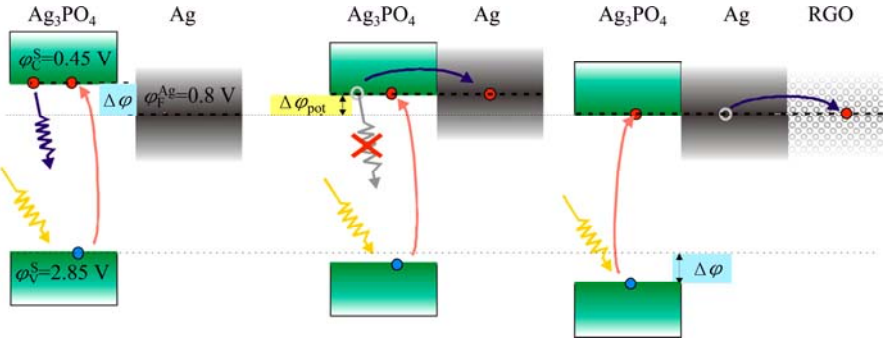

Fig. 9 Model explaining increase of activity of Ag_3PO_4 upon functionalization with Ag/AgBr and RGO [58]

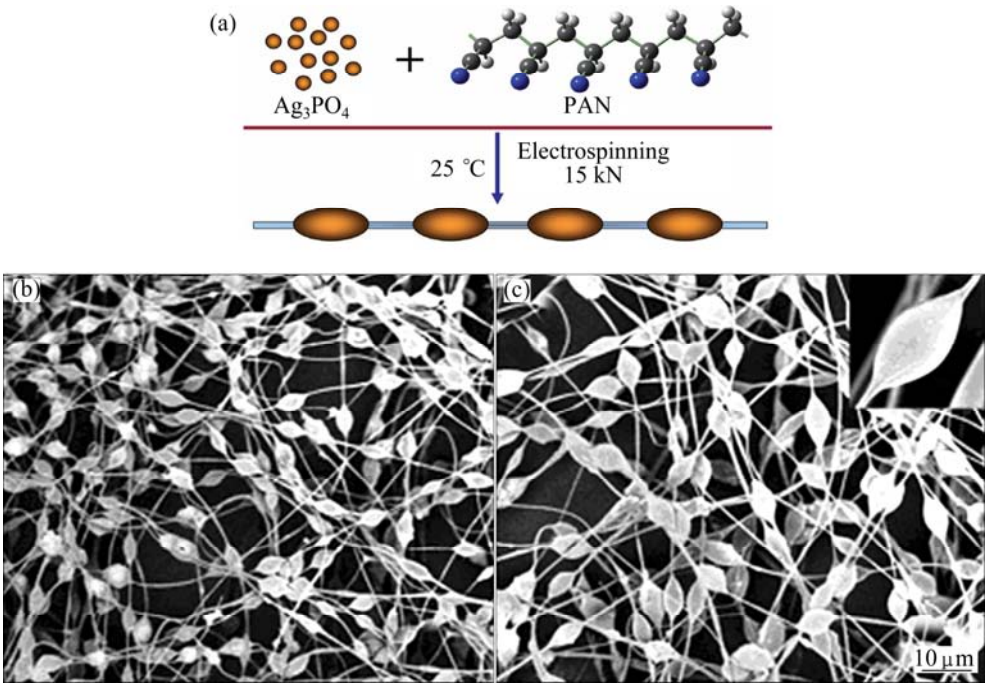

Fig. 10 Schematic illustration of formation process of Ag_3PO_4–PAN necklace-like nanofibers prepared by electrospinning (a) and SEM images of products (b, c) [59]

namely morphology control and hetero-structure construction, are employed to improve the activity and practicability of Ag_3PO_4 based photocatalysts, which are proved to be highly effective.

Future effort should be paid to: 1) the comparison between individual works in terms of activity of the catalysts; 2) development of novel preparation method which is environmental friendly and cost saving; 3) fabricating novel composites which possess high activity.

References

[1] HOFFMANN M R, MARTIN S T, CHOI W, BAHNEMANN D W. Environmental applications of semiconductor photocatalysis [J]. Chemical Reviews, 1995, 95(1): 69−96.

[2] SCHWARZENBACH R P, EGLI T, HOFSTETTER T B, von GUNTEN U, WEHRLI B. Global water pollution and human health [J]. Annual Review of Environment and Resources, 2010, 35: 109−136.

[3] RIFE R, THOMAS T, NORBERG D, FOURNIER R, RINKER F, BONOMO M. Chemical demilitarization: Disposing of the most hazardous wastes [J]. Environmental Progress, 1989, 8(3): 167−175.

[4] TONG H, OUYANG S, BI Y, UMEZAWA N, OSHIKIRI M, YE J. Nano-photocatalytic materials: Possibilities and challenges [J]. Advanced Materials, 2012, 24(2): 229−251.

[5] FUJISHIMA A. Electrochemical photolysis of water at a semiconductor electrode [J]. Nature, 1972, 238: 37−38.

[6] FOX M A, DULAY M T. Heterogeneous photocatalysis [J]. Chemical Reviews, 1993, 93(1): 341−357.

[7] LEGRINI O, OLIVEROS E, BRAUN A. Photochemical processes for water treatment [J]. Chemical Reviews, 1993, 93(2): 671−698.

[8] RAVELLI D, DONDI D, FAGNONI M, ALBINI A. Photocatalysis—A multi-faceted concept for green chemistry [J]. Chemical Society Reviews, 2009, 38(7): 1999−2011.

[9] ADDAMO M, AUGUGLIARO V, DI PAOLA A, GARCA L, PEZ E, LODDO V, MARC G, MOLINARI R, PALMISANO L, SCHIAVELLO M. Preparation, characterization, and photoactivity of polycrystalline nanostructured TiO_2 catalystsn [J]. Journal of Physical Chemistry B, 2004, 108(10): 3303−3310.

[10] KOMINAMI H, MURAKAMI S Y, KATO J I, KERA Y, OHTANI B. Correlation between some physical properties of titanium dioxide particles and their photocatalytic activity for some probe reactions in aqueous systems [J]. Journal of Physical Chemistry B, 2002, 106(40): 10501−10507.

[11] YU J C, ZHANG L, ZHENG Z, ZHAO J. Synthesis and characterization of phosphated mesoporous titanium dioxide with high photocatalytic activity [J]. Chemistry of Materials, 2003, 15(11): 2280−2286.

[12] SAKTHIVEL S, KISCH H. Daylight photocatalysis by carbon-modified titanium dioxide [J]. Angewandte Chemie International Edition, 2003, 42(40): 4908−4911.

[13] KHAN S U, AL-SHAHRY M, INGLER W B. Efficient photochemical water splitting by a chemically modified n-TiO_2 [J]. Science, 2002, 297(5590): 2243−2245.

[14] ASAHI R, MORIKAWA T, OHWAKI T, AOKI K, TAGA Y. Visible-light photocatalysis in nitrogen-doped titanium oxides [J]. Science, 2001, 293(5528): 269−271.

[15] YIN S, YAMAKI H, KOMATSU M, ZHANG Q, WANG J, TANG Q, SAITO F, SATO T. Preparation of nitrogen-doped titania with high visible light induced photocatalytic activity by mechanochemical reaction of titania and hexamethylenetetramine [J]. Journal of Materials Chemistry, 2003, 13(12): 2996−3001.

[16] LIVRAGHI S, VOTTA A, PAGANINI M C, GIAMELLO E. The nature of paramagnetic species in nitrogen doped TiO_2 active in visible light photocatalysis [J]. Chemical Communications, 2005, 41(1): 498−500.

[17] CAO S W, ZHU Y J. Hierarchically nanostructured α-Fe_2O_3 hollow spheres: Preparation, growth mechanism, photocatalytic property,

and application in water treatment [J]. Journal of Physical Chemistry C, 2008, 112(16): 6253−6257.

[18] LI L, KRISSANASAERANEE M, PATTINSON S W, STEFIK M, WIESNER U, STEINER U, EDER D. Enhanced photocatalytic properties in well-ordered mesoporous WO_3 [J]. Chemical Communications, 2010, 46(40): 7620−7622.

[19] WU S, CAO H, YIN S, LIU X, ZHANG X. Amino acid-assisted hydrothermal synthesis and photocatalysis of SnO_2 nanocrystals [J]. Journal of Physical Chemistry C, 2009, 113(41): 17893−17898.

[20] ANANDAN S, LEE G J, CHEN P K, FAN C, WU J J. Removal of orange II dye in water by visible light assisted photocatalytic ozonation using Bi_2O_3 and Au/Bi_2O_3 nanorods [J]. Industrial & Engineering Chemistry Research, 2010, 49(20): 9729−9737.

[21] SHANG M, WANG W, SUN S, ZHOU L, ZHANG L. Bi_2WO_6 nanocrystals with high photocatalytic activities under visible light [J]. Journal of Physical Chemistry C, 2008, 112(28): 10407−10411.

[22] DUNKLE S S, HELMICH R J, SUSLICK K S. $BiVO_4$ as a visible-light photocatalyst prepared by ultrasonic spray pyrolysis [J]. Journal of Physical Chemistry C, 2009, 113(28): 11980−11983.

[23] TANG J, ZOU Z, YE J. Efficient photocatalytic decomposition of organic contaminants over $CaBi_2O_4$ under visible-light irradiation [J]. Angewandte Chemie International Edition, 2004, 43(34): 4463−4466.

[24] AI Z, ZHANG L, LEE S. Efficient visible light photocatalytic oxidation of NO on aerosol flow-synthesized nanocrystalline $InVO_4$ hollow microspheres [J]. Journal of Physical Chemistry C, 2010, 114(43): 18594−18600.

[25] MAEDA K, TAKATA T, HARA M, SAITO N, INOUE Y, KOBAYASHI H, DOMEN K. GaN: ZnO solid solution as a photocatalyst for visible-light-driven overall water splitting [J]. Journal of the American Chemical Society, 2005, 127(23): 8286−8287.

[26] LI G, KAKO T, WANG D, ZOU Z, YE J. Composition dependence of the photophysical and photocatalytic properties of $(AgNbO_3)_{1-x}(NaNbO_3)_x$ solid solutions [J]. Journal of Solid State Chemistry, 2007, 180(10): 2845−2850.

[27] ZOU Z, ARAKAWA H, YE J. Substitution effect of Ta^{5+} by Nb^{5+} on photocatalytic, photophysical, and structural properties of $BiTa_{1-x}Nb_xO_4$ ($0\leq x\leq 1.0$) [J]. Journal of Materials Research, 2002, 17(6): 1446−1454.

[28] UMEZAWA N, SHUXIN O, YE J. Theoretical study of high photocatalytic performance of Ag_3PO_4 [J]. Physical Review B, 2011, 83(3): 035202.

[29] OUYANG S, ZHANG H, LI D, YU T, YE J, ZOU Z. Electronic structure and photocatalytic characterization of a novel photocatalyst $AgAlO_2$ [J]. Journal of Physical Chemistry B, 2006, 110(24): 11677−11682.

[30] MARUYAMA Y, IRIE H, HASHIMOTO K. Visible light sensitive photocatalyst, delafossite structured α-$AgGaO_2$ [J]. Journal of Physical Chemistry B, 2006, 110(46): 23274−23278.

[31] YI Z, YE J, KIKUGAWA N, KAKO T, OUYANG S, STUART-WILLIAMS H, YANG H, CAO J, LUO W, LI Z. An orthophosphate semiconductor with photooxidation properties under visible-light irradiation [J]. Nature Materials, 2010, 9(7): 559−564.

[32] NG H, CALVO C, FAGGIANI R. A new investigation of the structure of silver orthophosphate [J]. Acta Crystallographica Section B: Structural Crystallography and Crystal Chemistry, 1978, 34(3): 898−899.

[33] MA X, LU B, LI D, SHI R, PAN C, ZHU Y. Origin of photocatalytic activation of silver orthophosphate from first-principles [J]. Journal of Physical Chemistry C, 2011, 115(11): 4680−4687.

[34] MASSE R, TORDJMAN I, DURIF A. Affinement de la structure cristalline du monophosphate d'argent Ag_3PO_4: Existence d'une forme haute témperature [J]. Zeitschrift für Kristallographie, 1976, 144(1−6): 76−81.

[35] LIU J J, FU X L, CHEN S F, ZHU Y F. Electronic structure and optical properties of Ag_3PO_4 photocatalyst calculated by hybrid density functional method [J]. Applied Physics Letters, 2011, 99(19): 191903.

[36] DONG P, WANG Y, LI H, LI H, MA X, HAN L. Shape-controllable synthesis and morphology-dependent photocatalytic properties of Ag_3PO_4 crystals [J]. J Mater Chem A, 2013, 1(15): 4651−4656.

[37] LIU J K, LUO C X, WANG J D, YANG X H, ZHONG X H. Controlled synthesis of silver phosphate crystals with high photocatalytic activity and bacteriostatic activity [J]. Cryst Eng Comm, 2012, 14(24): 8714−8721.

[38] LIANG Q, MA W, SHI Y, LI Z, YANG X. Hierarchical Ag_3PO_4 porous microcubes with enhanced photocatalytic properties synthesized with the assistance of trisodium citrate [J]. Cryst Eng Comm, 2012, 14(8): 2966−2973.

[39] BI Y, OUYANG S, UMEZAWA N, CAO J, YE J. Facet effect of single-crystalline Ag_3PO_4 sub-microcrystals on photocatalytic properties [J]. Journal of the American Chemical Society, 2011, 133(17): 6490−6492.

[40] HU H, JIAO Z, YU H, LU G, YE J, BI Y. Facile synthesis of tetrahedral Ag_3PO_4 submicro-crystals with enhanced photocatalytic properties [J]. J Mater Chem A, 2013, 1(7): 2387−2390.

[41] XU Y S, ZHANG W. Morphology-controlled synthesis of Ag_3PO_4 microcrystals for high performance photocatalysis [J]. Cryst Eng Comm, 2013, 15(27): 5407−5411.

[42] QUE R. High-yield synthesized silver orthophosphate nanowires and their application in photoswitch [J]. Frontiers of Optoelectronics in China, 2011, 4(2): 176−180.

[43] WANG J, TENG F, CHEN M, XU J, SONG Y, ZHOU X. Facile synthesis of novel Ag_3PO_4 tetrapods and the {110} facets-dominated photocatalytic activity [J]. Cryst Eng Comm, 2012, 15(1): 39−42.

[44] JIAO Z, ZHANG Y, YU H, LU G, YE J, BI Y. Concave trisoctahedral Ag_3PO_4 microcrystals with high-index facets and enhanced photocatalytic properties [J]. Chemical Communications, 2013, 49(6): 636−638.

[45] SKRABALAK S E, XIA Y. Pushing nanocrystal synthesis toward nanomanufacturing [J]. ACS Nano, 2009, 3(1): 10−15.

[46] LOU Z, HUANG B, WANG Z, ZHANG R, YANG Y, QIN X, ZHANG X, DAI Y. Fast-generation of Ag_3PO_4 concave microcrystals from electrochemical oxidation of bulk silver sheet [J]. Cryst Eng Comm, 2013, 15(25): 5070−5075.

[47] WANG H, HE L, WANG L, HU P, GUO L, HAN X, LI J. Facile synthesis of Ag_3PO_4 tetrapod microcrystals with an increased percentage of exposed {110} facets and highly efficient photocatalytic properties [J]. Cryst Eng Comm, 2012, 14(24): 8342−8344.

[48] YAO W, ZHANG B, HUANG C, MA C, SONG X, XU Q. Synthesis and characterization of high efficiency and stable Ag_3PO_4/TiO_2 visible light photocatalyst for the degradation of methylene blue and rhodamine B solutions [J]. Journal of Materials Chemistry, 2012, 22(9): 4050−4055.

[49] LI G, MAO L. Magnetically separable Fe_3O_4–Ag_3PO_4 sub-micrometre composite: Facile synthesis, high visible light-driven photocatalytic efficiency, and good recyclability [J]. RSC Advances, 2012, 2(12): 5108−5111.

[50] GUO J, OUYANG S, ZHOU H, KAKO T, YE J. $Ag_3PO_4/In(OH)_3$ composite photocatalysts with adjustable surface-electric property for efficient photodegradation of organic dyes under simulated solar-light irradiation [J]. Journal of Physical Chemistry C, 2013, 117(34): 17716−17724.

[51] ZHAI W, LI G, YU P, YANG L, MAO L. Silver phosphate/carbon nanotube-stabilized pickering emulsion for highly efficient photocatalysis [J]. Journal of Physical Chemistry C, 2013, 117(29):

15183−15191.

[52] YANG X, CUI H, LI Y, QIN J, ZHANG R, TANG H. Fabrication of Ag_3PO_4-graphene composites with highly efficient and stable visible light photocatalytic performance [J]. ACS Catalysis, 2013, 3(3): 363−369.

[53] TANG J, GONG W, CAI T, XIE T, DENG C, PENG Z, DENG Q. Novel visible light responsive Ag@(Ag_2S/Ag_3PO_4) photocatalysts: Synergistic effect between Ag and Ag_2S for their enhanced photocatalytic activity [J]. RSC Advances, 2013, 3(8): 2543−2547.

[54] LEE I, ALBITER M A, ZHANG Q, GE J, YIN Y, ZAERA F. New nanostructured heterogeneous catalysts with increased selectivity and stability [J]. Physical Chemistry Chemical Physics, 2011, 13(7): 2449−2456.

[55] BI Y, OUYANG S, CAO J, YE J. Facile synthesis of rhombic dodecahedral AgX/Ag_3PO_4 (X=Cl,Br,I) heterocrystals with enhanced photocatalytic properties and stabilities [J]. Physical Chemistry Chemical Physics, 2011, 13(21): 10071−10075.

[56] ZHANG H, HUANG H, MING H, LI H, ZHANG L, LIU Y, KANG Z. Carbon quantum dots/Ag_3PO_4 complex photocatalysts with enhanced photocatalytic activity and stability under visible light [J]. Journal of Materials Chemistry, 2012, 22(21): 10501−10506.

[57] KUMAR S, SURENDAR T, BARUAH A, SHANKER V. Synthesis of a novel and stable g-C_3N_4–Ag_3PO_4 hybrid nanocomposite photocatalyst and study of the photocatalytic activity under visible light irradiation [J]. J Mater Chem A, 2013, 1(17): 5333−5340.

[58] HOU Y, ZUO F, MA Q, WANG C, BARTELS L, FENG P. Ag_3PO_4 oxygen evolution photocatalyst employing synergistic action of Ag/AgBr nanoparticles and graphene sheets [J]. Journal of Physical Chemistry C, 2012, 116(38): 20132−20139.

[59] YU H C, JIAO Z G, HU H Y, LU G X, YE J H, BI Y P. Fabrication of Ag_3PO_4/PAN composite nanofibers for photocatalytic applications [J]. Cryst Eng Comm, 2013, 15: 4802−4805.

Ag_3PO_4体系光催化材料的研究进展：基础与改性

马运柱，成 帆，刘文胜，王 娟，王依锴

中南大学 粉末冶金国家重点实验室，长沙 410083

摘 要：Ag_3PO_4是一种高效的光催化剂，因而受到了极大的关注。其高光催化活性归功于其内禀电子结构。采用形貌控制和纳米复合体构筑的方法提高其性能和实用性。综述 Ag_3PO_4 单晶的晶体结构、性能及其基础理论，并用一些典型例子来说明提高其光催化活性的主要策略，即形貌控制和纳米复合体的构筑。

关键词：Ag_3PO_4体系光催化剂；电子结构；形貌控制；异质结构构筑；制备；光催化活性

(Edited by Wei-ping CHEN)